REVIEW OF TELLURIUM RELEASE RATES FROM LWR FUEL ELEMENTS AND AEROSOL FORMATION FROM SILVER CONTROL ROD MATERIALS

R. A. Lorenz
E. C. Beahm
R. P. Wichner

Chemical Technology Division
Oak Ridge National Laboratory
Oak Ridge, Tennessee 37830

(An Informal Letter Report)

February 28, 1983

REVIEW OF TELLURIUM RELEASE RATES FROM LWR FUEL ELEMENTS AND FORMATION FROM SILVER CONTROL ROD MATERIALS

R. A. Lorenz
E. C. Beahm
R. P. Wichner

1. THE RELEASE OF FISSION PRODUCT TELLURIUM FROM LIGHT WATER REACTOR FUEL

1.1 Introduction

The history of tellurium release studies began with unclad UO_2 heated in inert or reducing atmospheres. These tests showed high release rates for fission product tellurium which we define as a rate within a factor of 2 of that of iodine. Similarly, we will here consider a low release rate to be one-tenth or less than that of iodine. Since cesium and iodine generally exhibit similar release rates from UO_2 at temperatures >1400°C, the same definitions could be made in terms of cesium releases.

When tests were made with Zircaloy cladding present, the observed tellurium release rates were significantly lower. This was not always the case when tests were run with Zircaloy-clad UO_2 in steam or steam–air mixtures. It was qualitatively recognized that the release of tellurium was lower when the atmospheric conditions were less oxidizing. In some tests samples of the cladding were examined and found to contain large amounts of tellurium. However, the parameters affecting tellurium release were never systematically investigated.

1.2 Postulated Tellurium Release Behavior

Detailed study of the experiment data has enabled us to construct the following semiquantitative behavior model. The rate of escape of tellurium from the UO_2 fuel itself is approximately equal to that of iodine over the temperature range 1200 to 2800°C. Although this equivalency was measured in hydrogen and inert atmospheres, we will presume that it also holds true for steam and steam–hydrogen atmospheres. When Zircaloy cladding is present, the cladding retains the tellurium and the release from the fuel rod is drastically reduced, typically by a factor of 30.

If the exposure conditions permit continued oxidation of the Zircaloy, the cladding will release the captured tellurium as the degree of oxidation approaches 100%. Experimental data indicate that the presence of stainless steel, at least at the higher temperatures of interest, does not affect the above postulated tellurium behavior.

The next section of this report reviews previously available test data in relation to the above qualitative behavior model. In Sect. 1.4 recently acquired information is reviewed.

1.3 Review of Earlier Experimental Results

1.3.1 Summary of tests with high tellurium release

Tests resulting in high tellurium release are summarized in Table 1. Parker's diffusion release tests show an effect of burnup. For the 4000 MWd/MT burnup samples, the I, Te, and Cs data were averaged together since the scatter of data and number of tests made it difficult to determine individual element releases. Fifteen additional tests were run with 1000 MWd/MT burnup UO_2 that released fission products generally between the 1 and 4000 MWd/MT samples. The release (vaporization) of UO_2 was not measured. In many of the small-scale long-term tests, the vaporization of UO_2 and other normally nonvolatile fission products such as Ce, Zr, and Ru is significant. This is especially true with Davies diffusion tests.

The tungsten resistor and ORR in-pile tests show that the presence of stainless steel cladding has little effect on overall tellurium release when fuel samples are heated to very high temperatures. Oxidation of stainless-steel clad UO_2 at very high temperatures also results in high tellurium release. Oxidation of unclad UO_2 in air at lower temperatures (ORNL-3981) does have an effect on the relative releases of iodine and tellurium. Their release rates depend both on the temperature and time or completeness of oxidation. Several ORR in-pile melting tests were run with Zircaloy-clad high-burnup UO_2. The tellurium data from these tests were not completed and published because of a change in program emphasis at the time.

Only three tests with Zircaloy-clad UO_2 showed high tellurium release. These are tests CMF 991S, the CDE tests, and test HI-2, all of which are discussed in separate sections of this report.

Table 1. Summary of tests with high release of Te

Experiment description	Test No.	Cladding	UO_2 mass (g)	Burnup (MWd/MT)	Atmosphere	Temperature (°C)	Time (min)	Amount released (%)									
								Xe, Kr	I	Te	Cs	Ba	Sr	Ru	Ce	Zr	UO_2
Diffusion;[a] Parker		None	7	1	He	1200	330	0.3	0.57	0.63	0.11		0.004	0.01			
						1600	330	2.3	6.0	12.0	1.5		0.2	1.0		0.01	
						2000	330	19.0	40.0	65.0	16.0	15.0	6.0	16.0		1.0	
Diffusion;[b] Parker		None	~1.5	4000	He	1200	330	1.4	6.5	6.5	6.5	0.2	0.04	0.01			
						1600	330	13.0	40.0	40.0	40.0	6.0	0.7	0.1			
						2000	330	80.0	84.0	84.0	84.0	60.0	30.0	3.0			
Diffusion;[c] Davies		None	~1.0	1	H_2	1600	120	0.2	0.5	2.0	0.5	0.1	0.05		<0.001		
		None	0.05	1	H_2	2050	144	20.0	17.0	49.0	12.0	16.0	14.0	13.0	5.5		7.0
Tungsten crucible;[d] Parker		None	2.0	1	He	2800	2	99.0	94.0	97.0	69.0	2.8	0.44	0.35	0.15		0.16
Tungsten resistor		None	39.0[e]	1	He	1800–2800	~2	50.0	30.0	42.0	41.0	4.3	1.2	0.4	<0.6		0.3
		S.S.	39.0[f]	1	He	1800–2800	~2	56.0	52.0	31.0	46.0	4.2	1.0	0.5	0.3		0.2
ORR in-pile[g]		S.S.	6.0	1	He	~2400	5		86.0	86.0	71.0				0.4		
					Air	~2400	5		68.0	72.0	53.0				0.11		

[a] From first draft NUREG-0772. Smoothed data, total of 28 tests.

[b] From first draft NUREG-0772. Smoothed data, total of 10 tests.

[c] AERE-R-4342. Each temperature average of three tests.

[d] ORNL-3981. Average of six tests.

[e] The Technology of Reactor Safety, Vol. 2. Average of three tests.

[f] The Technology of Reactor Safety, Vol. 2. One test.

[g] ORNL-3843. Average of three tests.

1.3.2 Summary of tests with low tellurium releases

Tests with low tellurium release (compared with iodine release) are listed in Table 2. A few core meltdown (CM) tests without tellurium are included for comparison purposes. All of these tests except CM-30 were made with Zircaloy-clad fuel; some contained stainless steel alongside the fuel pins. It appears that the Zircaloy cladding was only partially oxidized during the helium and low temperature steam tests.

The SASCHA tests generally ran for 5 to 10 min at temperature; the release quantities are calculated for 1 min in order to make rate comparisons easier. The release rates for air and steam atmospheres are similar. We believe that the oxidation of zirconium in the melt was incomplete because of the large mass of molten material located in the bottom of the crucible. Some SASCHA tests were heated by direct induction coupling with the Zircaloy and stainless steel in the miniature core sample. With this type of heating, the induction currents caused part of the melt to climb up the walls of the crucible thus allowing this material to be in close proximity to the air or steam flowing above the crucible. Other tests were heated indirectly from an induction-heated susceptor located just outside of the crucible. We do not know which heating method was used in the various tests and therefore cannot determine whether the difference in exposed melt surface area affected the oxidation of melted material and subsequent fission product release. A study (NUREG/CR-2182, Vol. 2, Appendix C) showed that the vaporization of structural material components in SASCHA tests agreed well with the vapor pressures of the elements. This indicates that oxidation was incomplete.

The core melt (CM) tests are also believed to have been run with incomplete oxidation of the melted material. Hydrogen generation measurements usually show ~80% oxidation of the zirconium. The low tellurium and ruthenium releases combined with high barium and strontium releases are interpreted as being indicative of reducing conditions in the melt. Test CM-30 with no zirconium present retained tellurium and ruthenium.

Two other tests with Zircaloy-clad UO_2 showed low tellurium release. Tests CMF 996H and CMF 992S are discussed in the following section.

Table 2. Summary of tests with low release of Te

Experiment description	Test No.	Cladding	UO_2 mass (g)	Burnup (MWd/MT)	Atmosphere	Temperature (°C)	Time (min)	Amount released (%)									
								Xe, Kr	I	Te	Cs	Ba	Sr	Ru	Ce	Zr	UO_2
Tungsten resistor[a]		Zr	39	1	He	1800–2800	~2	46.0	35.0	0.8	30.0	9.0	10.0	0.15	0.5		0.06
Seven-rod TREAT[b] LOCA	FRF-2	Zr	5350	2800	Steam + He	1300	~2	0.48	0.12	$\sim 10^{-5}$	0.29				2×10^{-6}		2×10^{-5}
SASCHA simulant[c]		Zr	100	40,000 sim.	Air	1900	1		~90.0	0.75	7.5						
						2400[d]	1		92.0	5.8	73.0	0.1		0.0025	0.001	2×10^{-4}	
SASCHA simulant[e]		Zr	100	40,000 sim.	Steam	1900	1			1.6							
						2400	1		92.0	7.1	73.0	5.0		0.001	0.001	0.001	0.02
Bundle simulant; Parker	CM-20[f]	Zr		16,500 sim.	Steam + Ar	~2400	~8			<1.0				<1.0			1.3×10^{-4}
	CM-21[g]	Zr	625		Steam + Ar	2400	8			<1.0				<1.0			2×10^{-3}
	CM-19[f]	Zr	501		Steam + Ar	2400	8					9.3	12.7				10^{-5}
	CM-18[f]	Zr	966		Steam + Ar	2400	8										2×10^{-6}
	CM-23[h]	Zr			Steam + Ar	~2400	8					4.0	3.0				10^{-4}
	CM-16[i]	Zr	481		Steam + Ar	2400	8										10^{-3}
	CM-30[j]	S.S.			Steam + Ar	2400	8			<1.0				<1.0			
LOCA simulant; Lorenz		Zr		15,000 sim.	Steam + He	500–1300	10–1200		10.0	1.0							

[a] ORNL-3401. Data updated. Average of two tests.

[b] Nucl. Technol. V.11, August 1971, and ORNL-4710. UO_2 mass of seven rods.

[c] Sun Valley, Idaho, 1981.

[d] Iodine and cesium obtained by extrapolation of data by Lorenz.

[e] Columbus, Ohio, November 1981.

[f] NUREG/CR-2809, Vol. 1.

[g] NUREG/CR-2809, Vol. 2.

[h] NUREG/CR-2809, Vol. 3.

[i] NUREG/CR-2299, Vol. 4.

[j] G. W. Parker, personal communication, Feb. 14, 1983.

1.3.3 Summary of tests in the containment mockup facility (CMF) and containment research installation (CRI)

Pertinent test data from CMF and CRI runs are shown in Table 3. The fuel specimens in these tests were heated at the melting point for ~2 min. Steam or air flow was adequate for complete oxidation, but the melt geometry may have prevented complete oxidation during the short heating period. When Zircaloy was used, the melt often sparked during cooldown, especially if air was admitted, an indication that oxidation was not yet complete.

Tests with stainless steel cladding indicated high tellurium release with the exception of CMF-990S. The Zircaloy-clad tests had tellurium releases ranging from high to low. For the highest tellurium release test, CMF 991S, severe oxidation was reported. The test with the lowest tellurium release, CMF 992S, did not include air in the gas flowing over the melted fuel.

The simulant tests used fission product simulants distributed uniformly through the pellets. Tellurium, ruthenium, and molybdenum powdered metals were mixed with UO_2 powder and the other simulants and cold pressed. The pellets were not sintered or heated in any way prior to the release tests. Melt residues were not examined for extent of oxidation after the tests.

1.3.4 Contamination/decontamination experiment (CDE) tests

Five tests were run in the CDE facility. Averages of the test results are given in Table 3. These tests were conducted at 22 psig, used short-cooled fuel, and were heated by high frequency induction. The fuel samples were placed on either 100 or 20 g of crushed UO_2 as an insulating base located in a 1-5/8-in.-ID quartz tube that was temperature controlled with circulated glycol at ~150°C. The steam flow was reported to be 1.6 ft/s "over the fuel" which translates to 63 L/min (STP) if the reference temperature is 150°C.

An unirradiated fuel sample was run and examined. The lower side of the melt mixture was not completely oxidized although there apparently was plenty of steam and more than enough time to assure complete oxidation. The amount of Zircaloy was not given, but for the size fuel pin used 5-10 L (STP)

Table 3. Release of Te in other tests

Experiment description	Test No.	Cladding	UO_2 mass (g)	Burnup (MWd/MT)	Atmosphere	Temperature (°C)	Time (min)	Amount released (%)										
								Xe, Kr	I	Te	Cs	Ba	Sr	Ru	Ce	Zr	UO_2	Pu
CMF/CRI; Parker	CMF 991S[a]	Zr	40	10,000 sim	Air	~2400	~2		100	45.7	8.2		0.04	0.89				
	CRI 114[b]	Zr	40	6,000	Air + steam	~2400	~2		73.5	15.8	20.7			2.2				
	CMF 996H[c]	Zr	40	7,000	Air + steam	~2400	~2		90.2	2.4	30.2		0.77	0.23				
	CMF 992S[d]	Zr	40	10,000 sim	Steam + He	~2400	~2		92.3	0.43	96.0			0.12				
	CMF 981H[e]	S.S.	40	7000	Air	~2400	~2		91.0	55.0	37.0		0.01	0.002			0.005	0.005
	CMF 995H[f]	S.S.	40	1000	Air + steam	~2400	~2		~100	31.7	48.2		0.07	0.32				
	CMF 990S[g]	S.S.	40	10,000 sim	Air	~2400	~2		~100	8.4	62.5		0.05	0.48				
Contamination/ decontamination experiment	CDE[h]	Zr	~70.0	800	Steam	~2000-2400	25		17.0	12.0	11.0	0.04	0.03	0.07		0.0001		
Seven-rod TREAT LOCA	FRF-1[i]	Zr	765	650	Steam + He	950	~2	0.094	0.19	>0.015	0.056				9×10^{-4}	2×10^{-4}		
TREAT transient	3[j]	S.S.	30	~10	Moist air	2800	~1		39.0	31.0	39.0	10.0	6.3	7.6	3.4	3.4	3.5	
	4[j]	S.S.	30	~10	Wet air	2800	~1		34.0	27.0	32.0	9.3	5.3	1.2	0.72	0.67	0.66	
	5[k]	S.S.	32	9	1000 psi steam	2700	~1	2.7	0.7	0.4	0.1	0.01	0.01	0.01	0.001	0.001	0.002	
	6z[k]	Zr	32	16	1000 psi steam	2700	~1		10.0	5.0	23.0	2.6	2.3	2.1	2.2	1.2	1.9	
	7[l]	S.S.	32	19	Water	>3000	~1		5.0	3.0	5.0	0.9	0.4	0.2	0.1	0.04	0.08	
	8z[l]	Zr	32	18	Water	>3000	~1		7.0	2.0	6.0	1.3	0.5	0.1	0.1	0.04	0.1	
	9[m]	S.S.	32	27	Water	>3000	~1		67.0	28.0	58.0	1.6	0.7	1.7	0.49	0.38	0.98	
	10z[m]	Zr	32	32	Water	>3000	~1		53.0	13.0	52.0	2.5	2.2	1.7	0.63	0.56	0.70	
	11z[n]	Zr	32	14	300 psi water	>3000	~1		26.0	2.6	18.0	0.8	0.6	0.23	0.14	0.09	0.11	
	12z[n]	Zr	32	11	2500 psi water	>3000	~1		22.0	7.6	22.0	1.4	1.1	0.45	0.44	0.20	0.18	

[a] ORNL/TM-2628. Severe oxidation of fuel specimen noted. Same test designated CFM 2-24 in ORNL-3843 and ORNL-3915.

[b] ORNL-4374.

[c] ORNL/TM-2628. Same test designated CMF 4-11 in ORNL-4071.

[d] ORNL/TM-2628. Same test designated CMF 3-25 in ORNL-3843 and ORNL-3915.

[e] ORNL/TM-2628. Same test designated CMF-C in ORNL-3691 and CMF 3-5 in ORNL-3776 and ORNL-3915.

[f] ORNL/TM-2628. Same test designated CMF 10-29 in ORNL-3915.

[g] ORNL/TM-2628. Same test designated CMF 12-9 in ORNL-3776, ORNL-3843, and ORNL-3915.

[h] IN-1172. Average of five tests. Fractional release of fission product Mo = 0.04.

[i] Nucl. Technol. V.11, August 1971 and ORNL-4635.

[j] ORNL-3691.

[k] ORNL-3843. In experiment 6z, the cladding contained 2.5% of the original I, 11% of original Te, 5% of original Cs, 13% Ru, and 7% UO_2.

[l] ORNL-3915.

[m] ORNL-4071.

[n] ORNL-4228.

of steam total should have been enough for complete oxidation. In test CDE-5 gas samples were taken at the furnace outlet. The calculated amount of hydrogen formed in 30 min was only 0.3 L (STP), an unbelievably small amount.

The releases shown in Table 3 are "releases from fuel and furnace." We believe that most of the fission products released in vapor form condensed on or reacted with the cool quartz furnace tube so that transport from the furnace was primarily as aerosol.

Even though we cannot evaluate the test conditions completely, it is clear that the conditions were favorable for complete oxidation of the Zircaloy. Ruthenium release was greater than barium and strontium, an indication that conditions at the fuel were oxidizing. Tellurium release was essentially the same as iodine as well as we can determine. This appears to be a result of complete oxidation of the cladding, but cannot be claimed to be a very convincing example. Fission product molybdenum release was 0.04%. No other tests have reported molybdenum release.

1.3.5 TREAT transient tests and test FRF-1

In the TREAT transient tests, fissioning in the pellets heated UO_2 to melting or near melting in less than 0.5 s. The cladding melted or occasionally fragmented. Various atmospheres were used as described in Table 3. The cooldown rate was not measured because the thermocouples were destroyed by the temperature transient. Fission product release was usually much less than in other melting tests because of the short heating time. Splattered fuel and cladding made it difficult to determine release from the fuel. High releases of Ce, Zr, and UO_2 are an indication of such conditions. Overall the stainless-steel clad specimens released somewhat more tellurium (relative to iodine) than did the Zircaloy clad samples. The ratio of iodine to tellurium release in stainless-steel clad tests was 1.6; the same ratio with Zircaloy cladding was 3.5. The low trapping efficiency for tellurium was probably a result of the poor contact between the melted fuel and cladding. The melting process was apparently violent, scattering melted cladding and fuel around the containment. Oxidation of the Zircaloy ranged from 41 to 55% based on the hydrogen formed.

Test FRF-1, Table 3, is inconclusive regarding the release of tellurium. The low temperature and short heating time preclude significant oxidation of zirconium. The rupture opening in the center irradiated rod was much larger in FRF-1 than in FRF-2 (Table 2).

1.4 Review of Recent Tellurium Release Data

1.4.1 High temperature fission product release test series

In the high temperature test series, high burnup commercial PWR fuel from the H. B. Robinson reactor was heated in steam at several different temperatures. Tellurium released from the 8-in.-long fuel rod segments was measured by Spark Source Mass Spectrometry (SSMS). Samples of material deposited at several locations in the thermal gradient tube and on or near the glass wool filter (parts of the apparatus used for collecting the released fission products) were obtained by using graphite electrodes to take smear or swipe samples in as representative a manner as possible. The electrodes were then placed individually in the SSMS and the smear deposits vaporized for mass number analysis. This technique is only good within a factor of 2 per measurement. Since only part of the system is smeared, the estimated total tellurium released is subject to an even larger possible error.

Data for the three HI series tests run to date are listed in Table 4.

Table 4. Tellurium release in HI series test[a]

Test No.	Temperature (°C)	Time (min)	I, Cs, Kr release (%)	Te release[b] (%)	Zircaloy oxidized (%)
HI-1	1400	30	1.8–2.8	0.3	40[c]
HI-2	1700	20	50	50–100	100[c]
HI-3	2000	20	55	0.6	~35[d]

[a] H. B. Robinson PWR fuel, 28,000 MWd/MT.
[b] Accuracy is within a factor of 2.
[c] Based on posttest metallographic examination.
[d] Based on amount of hydrogen formed. Steam supply limited maximum cladding oxidation to ~60%.

Even though the tellurium release amounts are only approximate, it is clear that much more tellurium was released in test HI-2 than in the other tests. The extent of oxidation of the Zircaloy was essentially complete in that test. The low oxidation fraction shown for test HI-3 is a result of the limited steam supply and the relocation of the Zircaloy after melting. The relationship between tellurium release and Zircaloy oxidation observed in these tests parallels similar behavior in other tests described above.

1.4.2 Tellurium Release from Core at TMI-2*

Tellurium samples from TMI-2. Determination of the Te concentration in a highly radioactive sample requires special analytical methods; therefore, the Te level of such samples is usually missed unless specifically searched for. The main difficulties are (1) interference from ^{125m}Te, which is a relatively short-lived daughter of ^{125}Sb and therefore an indicator of Sb (not Te) transport, and (2) very weak photons from the other radioactive Te nuclides which require specialized sample preparation and x-ray detection procedures.

Mass spectroscopy has been used on some samples to determine levels of the stable Te nuclides (^{126}Te, ^{128}Te, and ^{130}Te).

However, ^{129m}Te with the most prominant gamma, was seen in some early samples sent to ORNL. This prompted a special lookout for Te in many of the subsequent samples received at ORNL. In addition, some Te concentrations were reported in the primary coolant (NSAC-30) and in the containment building air samples (GEND-005).

Primary loop water (no solids). Results reported in NSAC-30 (Table B.2) based on analyses of early primary water samples (29 March and 10 April 1979) indicate that 8–12% of the I and Cs inventory was in the primary water, but only from 0.1 to 0.01% of the Te inventory. This may be due to either (1) low Te release from fuel, or (2) low solubility of the Te species in water.

A sample received at ORNL 21 June 1979 (anal. No. 73212) corroborates the NSAC-30 result. Corrected for decay to 28 March, this sample indicated

---

*Most of the TMI samples at ORNL were received and handled by D. O. Campbell of the Chemical Technology Division without whose assistance this section could not have been assembled.

that the primary water contained 0.014% of the Te inventory and from 12 to 17% of the I and Cs inventory. (In the ORNL sample, all the Te activity was associated with the glass container and none was in the water.)

The above determinations were based on ^{132}Te, which is the most prominant activity at short decay times but which soon dissappears ($T_{1/2}$ = 78.2 h).

Primary water sample with solids. Sample No. 73212, received at ORNL 19 June 1979, consisted of water plus solids. About 96% of the Te activity (here ^{129m}Te was used for analysis) was associated with the solids. Combining the water and the solids results yields the following:

Activity ratio in the samples corrected to 28 March 1979

	Measured	Whole core ratio from ORIGEN
$^{129m}Te/^{131}I$	0.035	0.034
$^{129m}Te/^{134}Cs$	2.9	15.0
$^{129m}Te/^{136}Cs$	2.1	3.8
$^{129m}Te/^{137}Cs$	0.70	2.9

Since there is no way of knowing whether or not the solids level in this sample was representative, only highly qualitative conclusions may be drawn. But it appears from this sample that Te release from fuel rods was roughly equal to that of I and Cs.

(Incidently, about 97% of the iodine activity was associated with the solids in this sample!?)

The "sump sludge sample". This sample from the containment building contained 13-mL water and 0.389-g solids. It was analyzed in December 1982 relying on mass spectrometry for the stable Te nuclides 126, 128, 130, and stable Cs nuclides, gamma spectroscopy for ^{137}Cs, and neutron activation for ^{127}I and ^{129}I. Again, preponderantly the I and Te were associated with the solids, while the major part of the Cs was in the water.

Combining water and solids results and also totaling the nuclides per element yields the following ratios:

Concentration ratio in "sump sludge"

	Measured	Whole core from ORIGEN
Te/I	0.78	1.7
Te/Cs	13.0	0.18

Again, the conclusions can only be highly qualitative since there is only one sample with no possible indication of how representative it is. But from the above we see roughly equivalent Te and I releases from the core and perhaps also Cs, with indication that the Te and I (but not Cs) associated preferentially with solids.

Results from the "painted" sample. "Plug 401," which was a painted steel disc of ~2 3/4 in. diam projecting into the containment building, was gamma-scanned at ORNL 29 August 1979. Assuming this disk was representative of the entire inner containment surface (assuming A = 2.2×10^8 cm^2) yields:

	Percent of core inventory on containment wall
^{127m}Te	0.045
^{129m}Te	0.12
^{131}I	1.8
^{134}Cs	0.0021
^{137}Cs	0.0016

Perhaps the only implication of this sample is the negative one that it does not indicate aggressive Te retention in the core region.

Containment building air sample. A containment building air sample, including associated suspended matter was acquired ~1 May 1980 and reported in GEND-005 (Table 14). These results include ^{129m}Te, ^{129}I, ^{134}Cs, and ^{137}Cs determinations, from which the following summary may be drawn:

1. The air contained 20 μCi ^{129m}Te, which represents 4×10^{-9} fraction of this nuclide projected at this time by ORIGEN.
2. The air sample indicated that ~3.2 μCi ^{129}I was in the containment air, which is ~1.4×10^{-5} fraction of the whole core level.

3. Both ^{134}Cs and ^{137}Cs sample results indicate an airborne level of $\sim 5 \times 10^{-11}$ of whole core inventory.

Thus these air samples indicate that the normalized level of airborne Te in the containment was intermediate between I (high) and Cs (low). Some of the iodine may have been in the organic iodide form.

Conclusions regarding Te release from the TMI core. One can perhaps state only the negative result that no proof is given here that Te was strongly retained in the core region.

On the other hand, there is some indication (referring to the "primary water plus solids" and "sump sludge" samples) that Te was released from the TMI core region to an approximately equal degree as I and Cs.

1.5 Tellurium — Metal Reactions

1.5.1 Tellurium reaction with stainless steel

Summary of experimental results. Tellurium reacts with stainless steels at temperatures as low as 673 K.[1] Three stages have been observed in this reaction.[1-3] Initially a nickel telluride layer, containing some iron, is formed on the surface of the metal. Then a chromium telluride layer forms between the metal and the outer nickel telluride layer. Finally, a single layer of chromium telluride forms as the chromium strips tellurium from the less stable nickel telluride. The result is a chromium telluride layer with residual nickel and iron on the surface.

The extent of the three-stage reaction sequence depends on temperature, reaction time, and alloy. Thus, in a test with 20% Cr/25% Ni/Nb stabilized stainless steel at a temperature of 1123 K, 0.1 mg Te/1 mm^2 steel reacted almost instantaneously (<<160 s).[2] Initially two reaction layers were observed; then after annealing for 50.5 h (1.8×10^5 s) only one layer, the chromium telluride, was observed. The reaction product thickness of approximately 25 μm was reported by three different investigators[1-3] for the reaction of Te with four different stainless alloys at 1023 K after 1-h exposure. The overall width of the reaction zone then does not appear to be sensitive to the alloy content. However, the relative amounts of Ni-Fe-telluride and Cr telluride appears to vary with alloy nickel content and perhaps with grain size.

Tellurium transport (stainless steel system). The Ni-Fe-telluride reaction layer is composed of a nickel telluride containing some iron. The analysis of Te transport related to reaction with stainless steel will focus on nickel telluride. Experimental results[1-3] show that this material forms first and is less stable than the Cr telluride obtained after annealing.

The nickel rich side of the Ni-Te phase diagram[5] shows a low melting temperature of 1278 K. Thus, above 1278 K there will be a combination of nickel and Ni-Te liquid. No studies have reported the rate of the tellurium–steel reaction under liquidus conditions but it must be extremely rapid.

More important for reactor accident studies, at high temperature the rate of sublimation of Te from the reaction zone will also increase. The expected result of the combination of reaction and resublimination of Te is that tellurium will transport down a temperature gradient. The rate of transport will then depend on the temperature gradient and the vapor pressure of Te_2.

The vapor pressure for the reaction:

$$NiTe\ (solid) \rightleftharpoons Ni\ (solid) + 0.5Te_2\ (gas) \qquad (1)$$

is reported as:[6]

$$\log_{(mm\ Hg)} P_{Te_2} = -12930/T + 11.91 \qquad (2)$$

at T = 923 - 1073 K. This equation converts to:

$$\ln_{atm} P_{Te_2} = -29772/T + 20.79\ . \qquad (3)$$

We have calculated the vapor pressure of Te_2 according to Eq. (1) from 600–800 K using thermodynamic data from the FACT program.[7] The resultant equation is:

$$\ln_{atm} P_{Te_2} = -27142/T + 17.98\ . \qquad (4)$$

There is a reasonably good correlation in the P_{Te_2} calculated by Eqs. (3) and (4). Thus, at 850 K, a temperature between the range of these equations, Eq. (3) gives 6.6×10^{-7} atm and Eq. (4) gives 8.7×10^{-7} atm.

Vapor pressures can be used to obtain useful estimates of the rate of Te_2 resublimation. Of course, evaluation of actual rates requires kinetic

studies, but from thermodynamics we can obtain the maximum rate using the Hertz-Langmuir equation:[8]

$$J_{atm} = \frac{P}{(2\pi MRT)^{1/2}} \qquad (5)$$

where

J_{max} = maximum flux from the surface (mol/cm^2 s),

M = molecular weight (g/mol),

R = gas constant (erg/mol K°),

T = temperature (K),

P = equilibrium pressure (dynes/cm^2).

Table 5 was calculated using pressures calculated from Eqs. (3) and (4) in the appropriate temperature ranges.

Table 5. Tellurium vapor pressure above NiTe and maximum Te_2 flux vs temperature

T(K)	J (mol/cm^2 s)	P* (atm)
600	1.65×10^{-13}	1.45×10^{-12}
700	9.77×10^{-11}	9.31×10^{-10}
800	1.16×10^{-8}	1.19×10^{-7}
900	4.25×10^{-7}	4.60×10^{-6}
1000	1.10×10^{-5}	1.26×10^{-4}
1073	8.26×10^{-5}	9.52×10^{-4}

Conclusions regarding Te reactions with stainless steel. Tellurium reacts readily with stainless steel components under isothermal equilibrium conditions. However, in an open system in a temperature gradient, the tellurium vapor pressure over nickel telluride should bring about resublimation of tellurium which would then migrate down the temperature gradient. Calculated values for the maximum rate of resublimation (Table 5) show a rapid increase with temperature.

The reaction with stainless steel and the desorption of tellurium should be relatively insensitive to oxidation effects. Chromium would be the first metal in this system to form an oxide. Nickel oxide would not

form unless significantly larger amounts of oxygen was available; and tellurium oxide has an oxygen potential of only -12 kcal/mol O_2 at 1500 K.[9]

1.5.2 Tellurium reaction with zirconium

Summary of Experimental Results. Tellurium reacts with zirconium at temperatures as low as 673 K.[10] Studies carried out over a temperature range of 923–1273 K, with Zircaloy-4, resulted in the formation of two bands of reaction products.[3] The outer band was rich zirconium and tellurium and the inner band was brittle and irregular in thickness; the inner band varied in thickness between 5–10 μm. Tin was distributed at the bottom of the inner band in a concentration higher than in the bulk. In another set of tests, these at lower temperatures 673–773 K, tellurium was reacted with both bare Zircaloy-4 and with prefilmed (0.6 μm-thick ZrO_{2-x}) specimens.[10] After 11-12 days (9.5×10^5–1.0×10^6 s) of exposure at 673 K tellurium deposition on bare metal was 28 mg/cm^2 and on the prefilmed metal it was 25 mg/cm^2. There was no mention in this study of two bands of tellurium containing reaction product. It is likely that the lower temperatures restricted migration of tellurium into the metal, and metal outward towards the tellurium.

Desorption studies were conducted on the prefilmed Zircaloy-4 specimen. The specimen was desorbed 49 h (1.8×10^5 s) at 673 K under continuous evacuation. During this period, the specimen lost about 20% of the tellurium adsorbed. In another study of the desorption of tellurium,[11] clad specimens containing fission product deposits were heated at 673, 923, and 1273 K for 5–7 h (1.8×10^4–2.5×10^4 s). Tellurium displayed thermal stability up to 1273 K. The apparent difference in desorption rates is again most likely due to the low temperature of the study cited from ref. 10. At 673 K the telluride formed should be $ZrTe_5$, at 1273 K the telluride would be $Zr_{1-x}Te$.

Tellurium transport. There are five different zirconium–tellurium compounds, Zr_5Te_4, ZrTe, $Zr_{1-x}Te$, $ZrTe_3$, and $ZrTe_5$.[12] The phase diagram for this system has not been studied in the zirconium-rich (>70 at. %) region. The compounds $ZrTe_4$, ZrTe, and $Zr_{1-x}Te$ are stable above 1000 K, the others are not. $Zr_{1-x}Te$ has a composition range between 52 and 66.6 at. % Te at 973 K. The liquidus temperature for this compound is about 1870 K. Not

surprisingly, liquidus temperatures on the tellurium-rich side of the phase diagram are much lower.

Tin forms a telluride with a nominal composition of SnTe and a homogeneity range of 50.1–51.1 at. % Te. This compound melts at 1077 K.[13]

Thermodynamic data have been estimated for $ZrTe_2$ and $ZrTe_3$.[9,14] The $ZrTe_2$ compound appears as $Zr_{1-x}Te$ in the most recent phase diagram for this system.[11] The free energy for the reaction:

$$Zr\ (solid) + 2Te\ (gas) \rightleftharpoons ZrTe_2\ (solid) \qquad (6)$$

is reported to be

$$\Delta G = -107500 + 40.13\ T \qquad (7)$$

at T = 298 – melting point of $ZrTe_2$. This data is based on an estimated heat of formation and entropy at 298 K.[14] The data at 298 K were assigned an uncertainty of ±28% for heat of formation. The uncertainty in ΔG values at higher temperatures would be even greater than at 298 K. Nevertheless, since this is the only data available for zirconium-tellurium compounds, it will be used to calculate tellurium vapor pressures with assumed uncertainty values of ±30% in the ΔG data.

The vapor pressure of Te_2 over $\langle ZrTe_2 \rangle$ calculated from Eq. (7) is given by:

$$\ln P_{\substack{Te_2 \\ atm}} = -54096/T + 20.194\ . \qquad (8)$$

Table 6 shows the maximum rate of vaporization of $Te_2(G)$ from $ZrTe_2$, calculated using the Hertz-Langmuir equation [Eq. (5)].

Table 6. Tellurium vapor pressure above $ZrTe_2$ and maximum $Te_2(g)$ flux vs temperature

T (K)	J (mol/cm^2 s)	P* (atm)
800	2.48×10^{-22}	2.53×10^{-21}
1000	1.66×10^{-16}	1.89×10^{-15}
1500	9.18×10^{-9}	1.28×10^{-7}

The values in Table 6 for $ZrTe_2$ may be compared to the values in Table 5 for NiTe. At 1000 K the maximum rate of $Te_2(g)$ vaporization is 10 orders of magnitude lower for vaporization from $ZrTe_2$. Due to uncertainty in the thermodynamic values for $ZrTe_2$, the value for $Te_2(G)$ flux could be in error, at 1000 K, by as much as ±5 orders of magnitude. However, even in the worst case of uncertainty, $Te_2(G)$ vaporization from $ZrTe_2$ is much less than from NiTe.

The vapor pressures of Te_2 over NiTe and $ZrTe_2$ are shown in Fig. 1 along with those of several other elements. Lower partial pressures can be expected as a result of alloy formation or solution in molten metals. As a point of reference, the fractional release rate of tellurium in SASCHA tests is usually found to be between those of tin and silver (NUREG/CR-2182, Vol. 2, Appendix C). The SASCHA tests consist of heating Zircaloy-clad UO_2-containing fission product simulants along with stainless steel to form a molten mixture in steam or air atmospheres.

Conclusions regarding Te reaction with Zr. Tellurium reacts readily with zirconium, even at temperatures as low as 673 K. At the higher temperatures expected in a nuclear reactor accident, the most likely phases to form are as follows: $Zr_{1-x}Te$ on the side of the clad exposed to tellurium and an inner phase of ZrTe, at temperatures up to 1273 K, above 1273 K the Zr_5Te phase. For calculations here, we have modeled the $Zr_{1-x}Te$ phase as $ZrTe_2$.

The calculations show that tellurium pressures over $ZrTe_2$ are much lower than over stainless steel at the same temperature.

The reaction of tellurium with zirconium and the desorption of tellurium may be sensitive to oxidation effects. Zirconium and tellurium have widely different oxygen potentials. At 1500 K, the oxygen potential for the formation of ZrO_2 is -195 kcal/mol O_2, and the oxygen potential for the formation of TeO_2 is -12 kcal/mol O_2.[9] Thermodynamic data for $ZrTe_2$ and ZrO_2 indicate that at 1500 K oxygen would replace tellurium in $ZrTe_2$ at oxygen potentials more positive than -171 kcal/mol O_2. Under conditions where oxidation of zirconium could occur, the tellurium released could either react with zirconium not yet oxidized, remain as liquid, or desorb.

Fig. 1

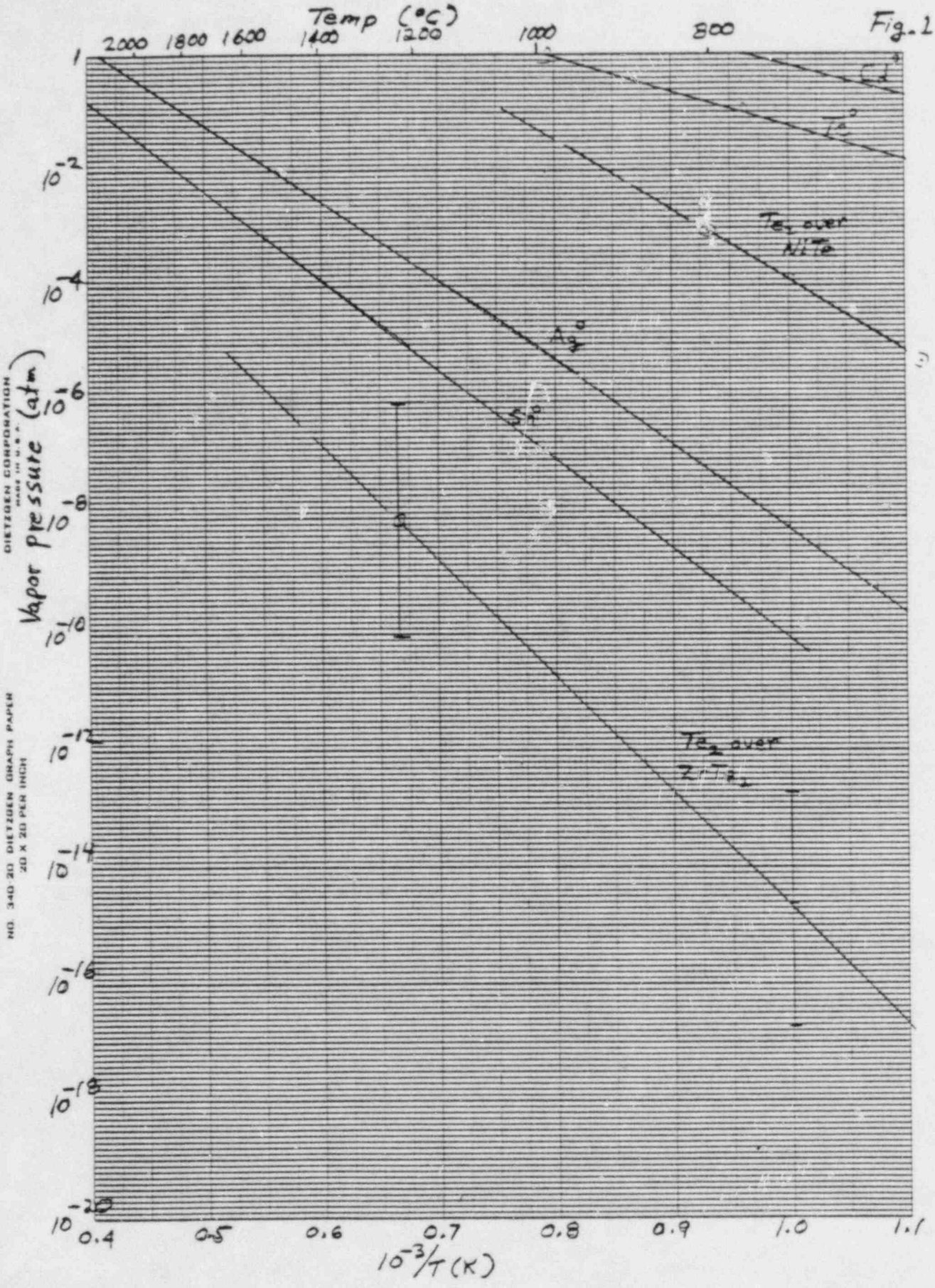
Temp (°C)
2000
1800
1600
1400
1200
1000
800
Vapor pressure (atm)
1
10^{-2}
10^{-4}
10^{-6}
10^{-8}
10^{-10}
10^{-12}
10^{-14}
10^{-16}
10^{-18}
10^{-20}
Te_2 over $NiTe_2$
Te_2 over $ZrTe_2$
0.4
0.5
0.6
0.7
0.8
0.9
1.0
1.1
$10^{-3}/T$ (K)
DIETZGEN CORPORATION
NO. 340 20 DIETZGEN GRAPH PAPER
20 X 20 PER INCH

Compounds of the type $ZrO_2 \cdot nTeO$, n = 2, 3 have been reported. There is no thermodynamic data for these compounds, but the oxygen potential for tellurium oxide indicates that oxygen pressures far in excess of those necessary to form ZrO_2 would be required before $ZrO_2 \cdot nTeO$ would form.

1.6 Oxidation of Zircaloy and its Effect on Tellurium

The oxidation of Zircaloy in steam occurs in a predictable manner below ~1500°C as a diffusion controlled process. An oxide layer (essentially ZrO_2) forms at the reaction surface. Oxygen diffuses through the oxide to form a layer of alpha zirconium adjacent to the oxide. Oxygen further diffuses into the original beta zirconium. With time the oxide and alpha layers grow in thickness until beta zirconium is eliminated entirely. The oxide layer continues to grow until the alpha layer is also consumed. Table 7 summarizes the oxidation of 0.0635-cm-thick Zircaloy at 1400°C in steam as calculated by the MULTRAN program. Two-sided oxidation is assumed to occur four times as fast as one-sided. The oxide and alpha layer thicknesses listed would be the sum of the two identical layers. The oxygen content of alpha zirconium at 1400°C levels out at ~0.4-atom oxygen per atom of zirconium.

Several tests have provided moderately convincing evidence that when Zircaloy becomes heavily oxidized the release of fission product tellurium is high. Test HI-2 was performed at 1700°C in steam. Posttest examination showed that the cladding was essentially 100% converted to ZrO_2 and mass spectrometry analysis showed high release of tellurium. Test CMF 991S heated Zircaloy-clad UO_2 to melting for ~2 min in air. Severe oxidation was reported and the tellurium simulant was released. The CDE tests exposed for 20 min in steam "at the fuel melting point" released tellurium almost as fast as iodine, but the actual test conditions and release amounts are not clearly understood. Samples from TMI-2 can be interpreted as showing significant tellurium release from the fuel.

The solubility of tellurium in zirconium and the formation of zirconium tellurides appear to be responsible for the good retention of tellurium in unoxidized Zircaloy cladding. The available thermodynamic data indicate that the tellurides in the cladding will not be decomposed until the cladding is essentially completely converted to ZrO_2. There is no guideline to estimate the rate of escape of tellurium caught between two layers of ZrO_2.

Table 7. Oxidation of 0.0635-cm-thick Zircaloy at 1400°C in steam

Reaction time (min)		Oxide layer		Alpha layer		Beta layer		Total weight gain (g/cm^2)	Percent conversion to ZrO_2
One-sided oxidation	Two-sided oxidation	Thickness (cm)	Oxygen conc. (g/cm^3)	Thickness (cm)	Oxygen conc. (g/cm^3)	Thickness (cm)	Oxygen conc. (g/cm^3)		
7.5	1.875	0.0046	1.39–1.51	0.0059	0.186–0.454	0.0545[a]	0.0087–0.0782	0.0093	6.5
30	7.5	0.0302	1.39–1.51	0.0433	0.299–0.454	0.0		0.0585	40.9
120	30.0	0.0717	1.39–1.51	0.0157	0.454[b]	0.0		0.1105	77.3
250	62.5	0.0953	1.51	0.0		0.0		0.143	100

[a]Beta layer disappears at ~21 min single-sided oxidation when the overall conversion to ZrO_2 is ~35% complete.

[b]The alpha layer reached near satuation at 80 min single-sided oxidation. The overall conversion to ZrO_2 was 64.7%. The alpha layer disappears at ~197 min single-sided oxidation when the oxidation conversion to ZrO_2 is ~96% complete.

A thin layer of oxide on the inner surface of the cladding does not seem to be a barrier to the pickup of tellurium. If the cladding balloons and ruptures with an opening sufficiently large to permit significant oxidation of the inner surface, a thick oxide layer could restrict the entry of tellurium. Only a small amount of cladding is needed to react with the tellurium since the Zr/Te atom ratio is ~700 for typical cladding and burnup of UO_2.

It is quite likely that with most of the induction-heated Zircaloy-clad fuel samples demonstrating low release of tellurium (SASCHA, CM series, CMF 992S, and CMF 996H) the rate of heatup was fast enough that the cladding melted before the inner surface was oxidized, thus allowing good contact between pellets and zirconium. It is possible that in some tests oxidation of the inner surface of the cladding did inhibit the pickup of tellurium (CRI-114). No quantitative data exist that show the rate of release of tellurium from zirconium as a result of oxidation of the zirconium.

In summary then, these observations appear to be consistent with the chemical considerations outlined in Sect. 1.6, namely: (1) the existence of dissolved Te in Zr or ZrTe formation does not greatly inhibit oxidation of Zr and (2) oxidation of Zr containing Te, either dissolved or as ZrTe, causes a large increase in Te vapor pressure and consequently rapid evolution.

1.7 Recommended Interim Tellurium Release Model

Obviously we do not know enough to prepare a detailed model of tellurium behavior. It does appear that tellurium release from the UO_2 pellets occurs approximately at the same rate as iodine release. However, when zirconium tellurides can form, the tellurium vaporization rate is reduced drastically. The effect of stainless steel mixed with melted Zircaloy cladding is believed to be essentially that of a diluent that thereby restricts the rate of oxidation of the zirconium and zirconium tellurides.

The question exists as to when zirconium tellurides are formed and when they are decomposed. Also what rates of release or vaporization exist for the two conditions? As stated previously, we believe that the existance of the low-volatility tellurides is related to the extent of oxidation of the

Zircaloy cladding. When single-sided oxidation occurs, tellurium might exist in the low volatility form until 96-100% conversion to ZrO_2 occurs (see Table 7). When two-sided oxidation occurs, especially if it is initiated before significant amounts of tellurium are released from the UO_2, much less oxidation might suffice to prevent formation of the low-volatility tellurides by providing a barrier for diffusion to the metal.

We propose the following model for tellurium release relative to iodine release for Zircaloy clad fuel. It applies to accidents in which the cladding fails so that oxidation occurs at the inner cladding surface at least to some extent.

1. When the local degree of cladding oxidation (i.e., in the control volume) is estimated as less than 90%, we recommend that a "low" Te release rate from the fuel plus cladding be employed, this "low" rate being equal to 1/40th of that of iodine.

2. When the local degree of cladding oxidation is predicted to reach or exceed 90%, we recommend use of a "high" release rate, equal to that of iodine. This "high" rate should be applied to both the Te inventory remaining in the pellet and also residing in the cladding.

The above is a gross simplification of what must actually occur. Keep in mind that the threshold for change in release rate is based on local cladding oxidation. Core average oxidation is an unacceptable substitute. If it is known that the local oxidation is being underestimated, it would be proper to compensate by reducing the changeover criterion to a lesser amount such as 70%. This might occur if single-sided oxidation is being calculated when it is known that the fuel rods have ballooned and ruptured thus allowing two-sided oxidation of the cladding.

The following expressions can be used to calculate the rate of release of tellurium from Zircaloy-clad fuel. They are based on the above model and on the iodine release rate functions presented in NUREG-0772 and in NUREG/CR-2182, Vol. 2.

With Zircaloy present and oxidation <90%, and for T (fuel temperature, °C) <1600°C:

$$k_r = 1.65 \times 10^{-10}\, e^{0.01061T} \qquad (9)$$

where

kr = fraction of tellurium released per minute from fuel and cladding.

For T >1600°C:

$$k_r = 9.04 \times 10^{-8} e^{5.22 \times 10^{-3}T} . \quad (10)$$

With Zircaloy oxidation >90% complete, and for T <1600°C:

$$k_r = 6.5 \times 10^{-10} e^{0.01061T} \quad (11)$$

for T >1600°C:

$$k_r = 3.616 \times 10^{-6} e^{5.22 \times 10^{-3}T} . \quad (12)$$

The above equations are plotted in Fig. 2. As in NUREG-0772, the fractional release rate constant, k_r, is based on the fraction remaining in the fuel and cladding at any instant.

2. AEROSOL FORMATION FROM SILVER CONTROL ROD MATERIALS

2.1 Mass in Core and General Behavior

Most PWRs contain silver control rod elements consisting of an alloy with composition 81 mol % Ag — 14 mol % In — 4.9 mol % Cd. The total mass is ~2800 kg, compared with ~16,500-kg Zircaloy, ~2000-kg stainless steel, and 79,700-kg UO_2. Thus the silver alloy makes up ~2.8% of the PWR core mass.

Observation in the Core Melt test facility at ORNL indicates that a rather energetic failure of stainless steel cladding occurs due to generation of internal pressure probably accompanied with some weakening of the stainless steel by the molten silver. The failure temperature is not known; but is probably lower than the ~1400°C point expected from steel softening alone.

In addition, it was observed that the molten silver alloy, released from the control rod in this fashion effectively wets Zircaloy. [In contrast, in tests with bare silver (no steel), no wetting of the Zircaloy occurred, and a different type of result was obtained.]

2.2 Ag-In-Cd Release in SASCHA Tests

Recent tests in the SASCHA facility at KfK included simulated control rod material. Silver release results from two recent tests in steam are shown in Fig. 3; a comparison is shown in this figure for fission-product silver from an earlier test.

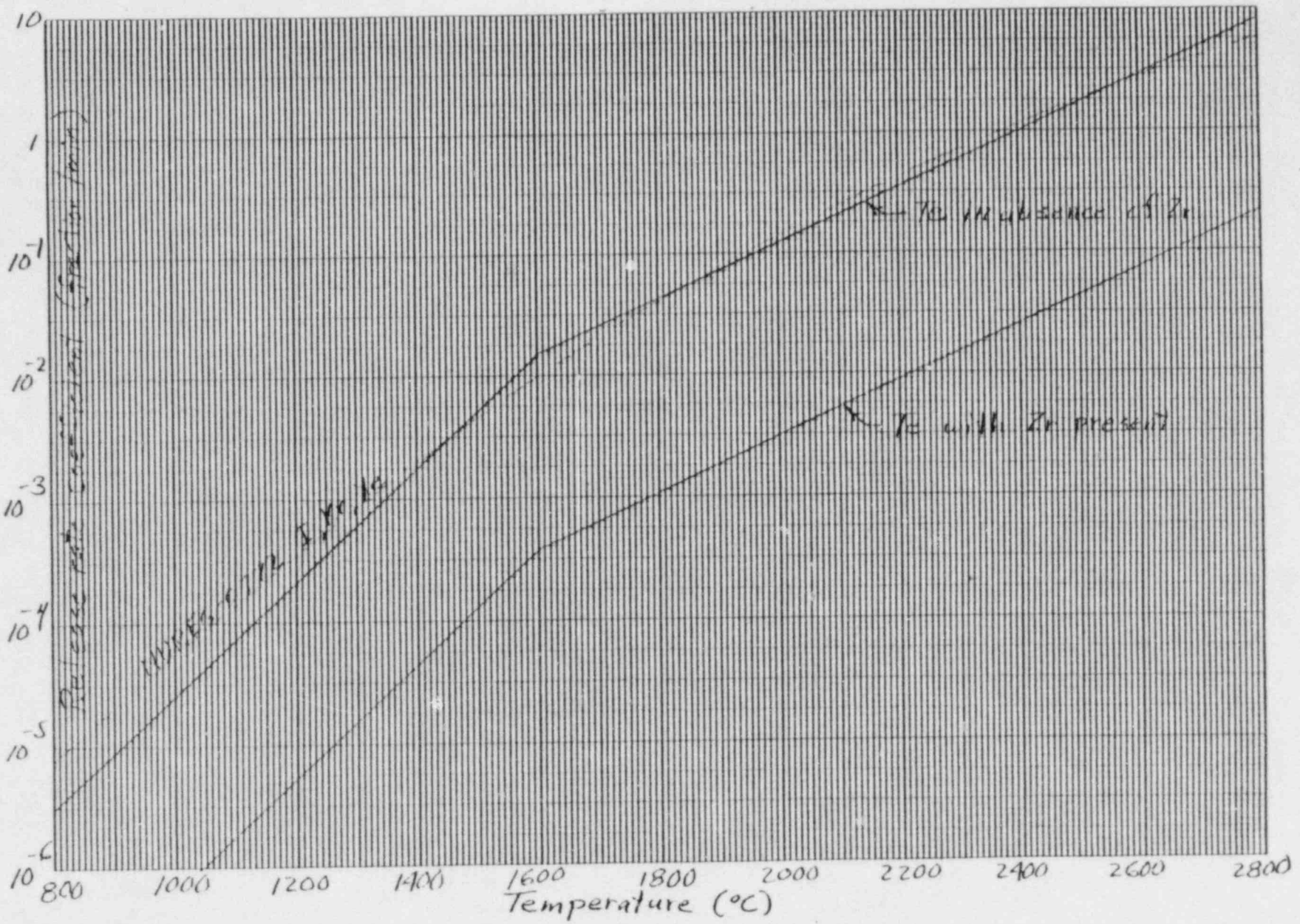

Fig. 2. Tellurium release rate coefficients.

Note, ~45% of the Ag was released from the absorber rod in the test at 2050°C. The release occurs within the first 5 min of the time at temperature. About ~80% of the Ag was released in the test at ~2200°C.

Also note that evolution rates of fission product silver appear to be comparable to control silver releases in the SASCHA tests.

Albrecht has calculated whole core releases of control rod material using his observed release rates for a particular core heatup history consisting of 15 min uniformly at 2200°C followed by 15 min at 2400°C for the slumped core. These calculated results are as follows:

Control rod material release from core from Albrecht using SASCHA data

	Percent release from core
Ag	75
In	20
Cd	100

2.3 Ag-In-Cd Release in Core-Melt Tests

Significantly lower control rod material releases are currently being observed by G. W. Parker in the 1-kg Core Melt Facility. These tests employ ~1 kg of representative core mass; however, the temperature distribution in these test samples are now well known.

Control rod material releases reported by Parker in 1-kg Core Melt Facility Tests

	Percent release from core
Ag	6.1
In	5.4
Cd	53.0

metallic form. In two test cases using MARCH currently being reviewed at ORNL, H_2/H_2O ratios in the reactor vessel were generally less than unity throughout most of the core heatup time. Based on this very limited view, it is judged that indium aerosol would, in contrast with Cd and Ag, likely to be the oxide, In_2O_3, rather than the metal.

2.5 Chemical and Metallurgical Considerations

Some important physical and chemical properties of these materials are given below:

	Melting point (°C)	Boiling point (°C)	H_2/H_2O ratio below which oxide forms
Ag	961	2163	Low
In	167	2073	~1
Cd	321	767	~0.01
Zr	1852	4409	High
In_2O_3			—
ZrO_2	2700		—

Since anticipated H_2/H_2O ratios may be in the range ~0.1 to ~1 (based on a very limited examination), we may expect that released Ag and Cd remain in the elemental form. On the other hand, released indium may be either elemental or as In_2O_3, since its H_2/H_2O transition is in the expected range.

In comparison, Zr is extremely oxygen acquisitive and will tend to become ZrO_2 at all except the most minute H_2/H_2O ratios.

We should also note that Cd° and In° are significantly more volatile than Ag° and thus have greater chance for vaporization and advection as a gas. However, indium oxidation, if it occurs, would greatly reduce its volatility.

Solubility in Zr. Examination of the Ag-Zr, In-Zr, and Cd-Zr binary phase diagrams indicates high solubility of Ag, In, and Cd in Zr.

Therefore, if conditions allow dissolution in Zr, the vapor pressure of these materials would be reduced approximately by its local mole fraction in the resulting alloy (Raoult's law).

However, such alloy formation would not inhibit Zr oxidation which involves far stronger chemical binding forces. In the event of Zr oxidation, any dissolved Ag, Cd, or In would exert its higher elemental vapor pressure.

As noted above, Zr oxidation conditions could possibly oxidize In as well, in which case the In vapor pressure would revert to a much lower level typical of the oxide.

2.6 Recommended Interim Release Estimate for Ag-In-Cd

It is apparent from the above that the release of control rod alloy from the core region involves complex physical and chemical processes requiring some care and modeling sophistication. In the interim we recommend the following procedure based upon the above discussion.

Recommended interim silver alloy release-from fuel model

1. Assume failure of the control rod cladding at T = 1400°C; i.e., when the maximum control-volume temperature along the rod reaches this value.
2. At the time of rod rupture, assume 5% of the Ag, 5% of the In, and 50% of the Cd becomes aerosol in the RV gas space.
3. Linearly increase the degree of release as the predicted local core temperature rises, such that as the melting point is reached, 50% of the Ag, 15% of the In, and 80% of the Cd in the control volume becomes aerosol.
4. If local temperatures are predicted to rise above the melting point (~2300°C), the balance of the control rod alloy materials should be released as 2800°C is reached.

3. REFERENCES

1. P. Hofmann, "Studies on the Reactivity of Steels with Simulated Fission Products in the Presence of UO_2, $(U,Pu)O_2$ and UC and Possible Ways of Improving the Compatibility Behavior of Oxide Fuel Pins," Report KfK-1831 (1974).

2. R. C. Lobb and I. H. Robins, "A Study of the 20% Cr/25% Ni/Nb Stabilized Stainless Steel — Tellurium Reaction," J. Nucl. Mater. 62, 50 (1976).

3. M. S. Anand and D. D. Pruthi, "Surface Reactions of Tellurium on Steel and Zircaloy 4," Report B.A.R.C. 1009 (1979).

4. O. Gotzmann, "A Thermodynamic Model for the Attack Behavior in Stainless Steel Clad Oxide Fuel Pins," J. Nucl. Mater. 84, 39 (1979).

5. K. O. Klepp and K. L. Komarek, "Transition Metal — Chalcogen System, III. The System Nickel — Tellurium," Monat. Chem. 103, 934 (1972).

6. D. M. Chizhikow and V. P. Shchastlwyi, Tellurium and the Tellurides, p. 256, Collet, London, 1970.

7. W. T. Thompson, C. W. Bale, and A. D. Pelton, "Interactive Computer Tabulation of Thermodynamic Properties with the F*A*C*T System," J. Metals , 18 (1980).

8. A. W. Searcy, D. V. Ragone, and U. Colombo, Chemical and Mechanical Behavior of Inorganic Materials, pp. 66-69, Wiley Interscience, 1970.

9. P. E. Blackburn and C. E. Johnson, "Light Water Reactor Fission Product Data Assessment," Report ANL-82-42 (1982).

10. J. M. Genco, W. E. Berry, H. S. Rosenberg, and D. L. Morrison, "Fission Product Deposition and Its Enhancement Under Reactor Accident Conditions: Deposition on Primary-System Surfaces," Report BMI-1863 (1969).

11. R. S. Forsyth, W. H. Blackadder, and B. Nilsson, "Volatile Fission Product Behavior in Reactor Fuel Rods Under Accident Conditions," p. 5 in Proceedings of the Behavior of Water Reactor Fuel Elements Under Accident Conditions, Part One, CSNI Report No. 13 (1976).

12. H. Sodeck, H. Mikler, and K. L. Komarek, "Transition Metal—Chalcogen Systems, VI: The Zirconium—Tellurium Phase Diagram," Monat. Chemie 110, 1 (1979).

13. F. A. Shunk, Constitution of Binary Alloys, 2nd Supplement, McGraw-Hill, New York, p. 688, 1969.

14. K. C. Mills, Thermodynamic Data for Inorganic Sulphides, Selenides, and Tellurides, Butterworths, London, p. 703, 1974.

15. R. P. Agarwala, E. Govindan, and M. C. Naik, Anal. Chem. 32, 720 (1960).

16. R. P. Agarwala, M. C. Naki, and J. Z. Shankar, Anorg. Algem. Chem. 307. 202-204 (1961).